JOURNAL OF MATERIALS SCIENCE 21 (1986) 705–710

High temperature mechanical properties of single phase alumina

ATUL H. CHOKSHI, JOHN R. PORTER
Department of Materials Science and Center for Electron Microscopy and Microanalysis, University of Southern California, Los Angeles, California 90089-0101 USA

The creep properties of a commercial, single phase alumina have been determined in the temperature range of 1623 to 1723 K. The stress exponent, n, in the relationship $\dot{\varepsilon} \propto \sigma^n$ was determined to be 1.9 and the true activation energy was found to be 635 kJ mol^{-1}. Normal primary stage creep transients were observed up to strains of 1%. At low stresses, steady-state conditions were not obtained due to the occurrence of concurrent grain growth. It is shown that the steady state creep results are consistent with the occurrence of an interface controlled diffusional creep mechanism.

1. Introduction

Structural ceramics are being increasingly exploited for applications at elevated temperatures and the creep performance, therefore, is critical in these materials. In general, the steady-state creep deformation of ceramic materials can be represented by an equation of the following form:

$$\dot{\varepsilon} = \frac{AGb}{kT} D_0 \exp\left[-Q/(RT)\right] (\boldsymbol{b}/d)^p (\sigma/G)^n \quad (1)$$

where $\dot{\varepsilon}$ is the strain rate, A is a dimensionless constant, G is the shear modulus, $\boldsymbol{b}$ is Burgers' vector, k is Boltzmann's constant, T is the absolute temperature, D_0 is the frequency factor, Q is the activation energy of the appropriate diffusion process, R is the gas constant, d is the grain size, p is the inverse grain size exponent, σ is the applied stress and n is the stress exponent.

The rate-controlling creep mechanisms are usually identified by comparing the theoretical and experimental values of Q, p and n. Reviews of the creep properties of fine grained alumina indicate that, under the experimental conditions typically used, $n \simeq 1$ to 2 and $p \simeq 2$ to 3 [1, 2]. However, the rate-controlling creep mechanisms have yet to be unambiguously identified; creep deformation has been variously identified to occur by diffusional creep processes [3], grain boundary sliding [4], a transition between diffusional creep and intragranular dislocation creep [5] and interface controlled diffusional creep mechanisms [6–8]. There are significant differences in the initial transients during the creep deformation of polycrystalline alumina and these have been tabulated recently by Cannon and Langdon [9]. It was noted that several studies reported a normal stage of primary creep during which the creep rate decreased with deformation and there were also some investigations in which a primary stage of creep was not detected. In addition, concurrent grain growth during creep deformation was noted in some studies on polycrystalline alumina [3, 6, 10].

There are clearly several discrepancies in the earlier studies of creep deformation of polycrystalline alumina. The present investigation on fine grained alumina was therefore undertaken with the following specific objectives. First, to examine the shape of the creep curves. Second, to study concurrent grain growth during creep deformation and to evaluate its effect on the shape of the creep curves. Third, to identify plausible rate-controlling mechanisms for steady state creep.

2. Experimental details

The commercially hot-pressed polycrystalline alumina chosen for this study was nominally doped with 0.25% MgO. Semiquantitative analyses of the as-received material are given in wt % as follows: C = 0.005, Si = 0.02, Mg = 0.35, Ca = 0.006, Fe = 0.02, Ni, Cu, Cr and Ti = trace and Ba < 0.001.

Scanning electron micrographs were obtained from a polished and thermally etched section of the as-received material. The spatial grain size, d, was determined to be 1.6 ± 0.15 μm. The spatial grain size was defined as $d = 1.74\bar{L}$, where $\bar{L}$ is the mean linear intercept grain size determined from 600 to 800 measurements. Inspection of the as-received material indicated that the grain size was uniform. Transmission electron microscopy studies did not reveal any glassy phase in the as-received material.

Creep specimens, having a nominal square cross-section of 3 mm × 3 mm, were deformed in four point flexure with an outer span of 19 mm and an inner span of 6.4 mm. The pivot points were made from high purity sapphire rods. During creep experiments, the displacement of the inner pivot points was monitored by a linear variable differential transducer in conjunction with a microcomputer. Typically, specimens were heated to the required temperature in a modified commercial high temperature furnace and the experimental set-up was allowed to stabilize for approximately 90 min before the commencement of creep tests.

0022–2461/86 $03.00 + .12

Nominally constant stress creep tests were performed in air at 1673 K to obtain information on the shape of the creep curves and the stress exponent. Creep experiments were also performed at 1623 and 1723 K to determine the activation energy for the rate-controlling creep process. Before creep deformation, the tensile faces of selected specimens were metallographically polished. After deformation, the tensile surfaces were lightly repolished and thermally etched to determine the final grain sizes. Stress and strain data were computed from the load–displacement data using the procedure developed by Hollenberg *et al.* [11].

3. Results

3.1. Shape of the creep curves

Fig. 1 is a plot of strain rate against strain for specimens tested at 1673 K and stresses between 6 and 150 MPa. It is noted that the creep curves exhibit a normal primary stage during which time the strain rate decreases with strain. Inspection of Fig. 1 indicates that at high stresses, well defined steady-state conditions are obtained for strains beyond approximately 2%. At lower stresses, however, there is no evidence of steady-state behaviour and it is noted that the strain rate continues to decline with increasing strain. It is relevant to note that at stresses greater than 50 MPa, the creep experiments involved testing times of less than approximately 2 h whereas the experiments performed at stresses of 19.8 and 6.2 MPa involved testing times of approximately 16 h and 112 h, respectively. The observed difference in steady-state behaviour at high stresses and low stresses is examined in Section 3.3 in terms of concurrent grain growth.

3.2. The stress exponent

The stress–strain rate data obtained from the above creep experiments are plotted on a logarithmic scale in Fig. 2. Data points for stresses of 50.5, 75.5 and 135 MPa correspond to steady-state behaviour. At stresses of 19.8 and 6.20 MPa, steady-state behaviour was not observed. The error bars indicated for these two stresses encompass the experimentally determined strain rates between strain levels of 2% and the strain levels corresponding to the respective terminations of the tests.

Inspection of Fig. 2 reveals that, at high stresses, the creep behaviour of polycrystalline alumina is associated with a stress exponent of 1.9. It is noted that at low stresses the strain rates at the end of the respective tests fall considerably below those anticipated from an extrapolation of the data at higher stresses. The Nabarro–Herring and Coble creep rates superimposed on to Fig. 2 are considered in Section 4.3.

3.3. Concurrent grain growth behaviour

It is apparent from an inspection of Equation 1 that, for a given stress and temperature, an increase in grain size would lead to a decrease in strain rate. Thus, the occurrence of grain growth could result in strain rates that decline with increasing strain. This possibility was examined by determining the final grain sizes of specimens deformed at stresses of 75.5, 19.8 and 6.20 MPa. The data obtained from this investigation are presented in Table I.

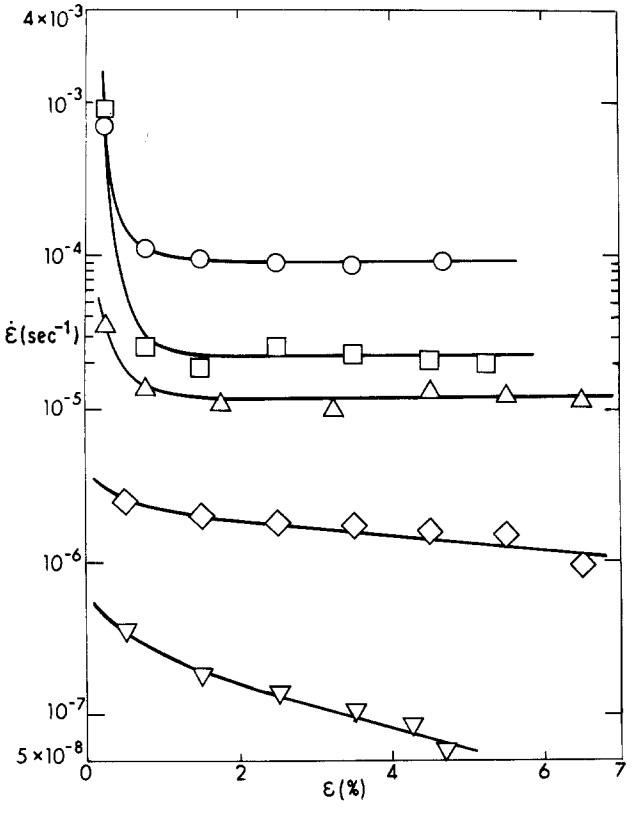

Figure 1 The variation of strain rate with strain for polycrystalline alumina deformed at a temperature of 1673 K, d = 1.6 μm. Values of strain rate, σ, (○) 135 MPa, (□) 75.5 MPa, (△) 50.7 MPa, (◇) 19.8 MPa and (▽) 6.20 MPa.

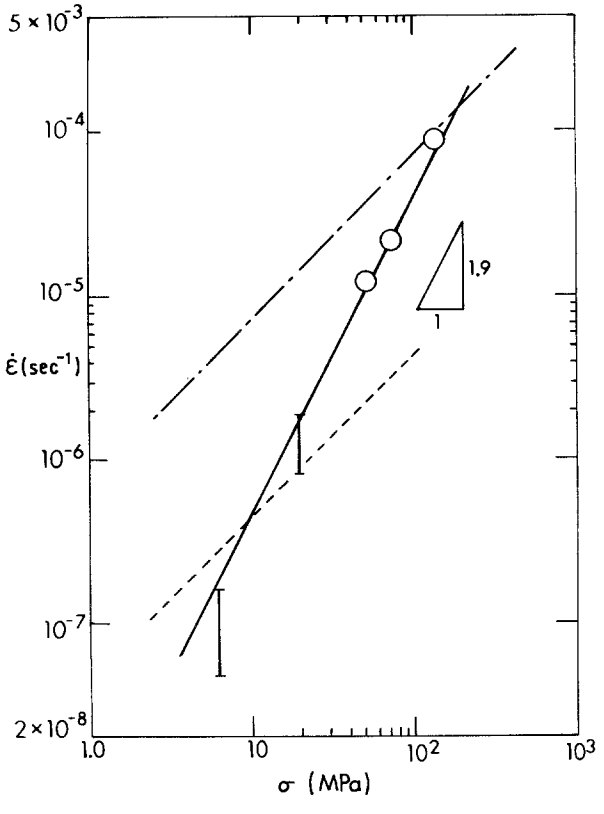

Figure 2 The stress–strain rate relationship for polycrystalline alumina deformed at a temperature of 1673 K, d = 1.6 μm. (– – –) Nabarro–Herring [14, 20], (– · – ·) Coble [22].

TABLE I Concurrent grain growth data

σ(MPa)	$\dot{\varepsilon}$(%)	t(sec)*	d(μm)
75.5	5.7	13278	1.7 ± 0.24
19.8	8.2	69950	2.3 ± 0.23
6.2	4.9	414000	2.8 ± 0.26

*The total time at 1673 K, including 1.5 h before creep testing and 1.5 h for thermally etching after creep testing.

Considerable grain growth had occurred in specimens deformed at stresses of 19.8 and 6.20 MPa, respectively, and there was almost no grain growth in the specimen tested at a stress of 75.5 MPa. In addition, a comparison of the final grain size in specimens deformed at stresses of 75.5 and 6.20 MPa to strains of 5.7 and 4.9%, respectively, suggests that grain growth is primarily a function of the time involved during individual elevated temperature tests.

3.4. Activation energy for creep deformation

The apparent activation energy for creep deformation was determined by performing experiments at a constant stress of 75.5 MPa and temperatures of 1623, 1673 and 1723 K, respectively. A short stage of primary creep was observed in all of these experiments. The steady-state creep rates obtained from these tests are plotted against $1/T$ in Fig. 3. Two creep experiments were performed at a temperature of 1623 K and a stress of 75.5 MPa, and these tests led to essentially identical steady-state creep rates. From the slope of the line in Fig. 3, the apparent activation energy was determined as 625 ± 70 kJ mol^{-1}.

4. Discussion

4.1. Shape of the creep curves

The observation of a primary creep region is indicative of some structural changes occurring during the initial stages of creep deformation. However, it is important to note that the extent of the primary creep region is limited to small strains of the order of $\simeq 1\%$. This is in contrast to primary stages extending to large strains of $\simeq 10\%$ during the creep deformation of large grained polycrystalline KBr [12]; the extensive primary stages were associated with the formation of sub-grains. The short primary stages observed in this study suggests that the sub-structure initially present in the material does not undergo significant change during the early stages of creep deformation. This is consistent with transmission electron microscopy studies of deformed specimens that reveal a lack of an increase in intragranular dislocation density and a lack of sub-grain formation [1, 13].

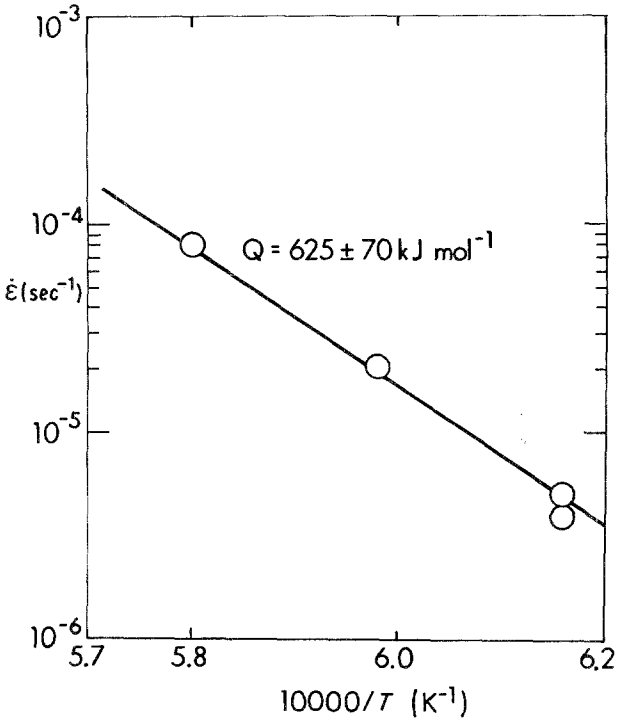

Figure 3 The variation in steady-state strain rate with reciprocal temperature for polycrystalline alumina deformed at 75.5 MPa. Q = 625 ± 70 kJmol^{-1}.

Steady-state diffusional creep deformation requires a uniform flux of vacancies along grain boundaries. Immediately upon loading a specimen, vacancy diffusion will occur more rapidly near intersections of grain boundaries owing to the relatively short diffusion paths [14, 15]. Consequently, a re-distribution of stress occurs during the initial stages of deformation, and this process leads to transients during diffusional creep [15]. Lifshits and Shikin [16] analysed transients during diffusional creep and they determined that the characteristic times for the decay of transients are independent of the applied stress. However, inspection of Fig. 1 indicates that, since the primary creep region involved an essentially constant strain level of $\simeq 1\%$, the time periods involved in the transient stage depend on the applied stress.

Heuer *et al.* [1] noted that concurrent grain growth during deformation could lead to the occurrence of a transient stage of creep. However, the data obtained in the present study are not in accordance with the above suggestion. Inspection of Fig. 1 indicates that, for a stress of 75.5 MPa, steady-state creep deformation is preceded by a short primary stage of creep, although examination of the specimen after creep deformation revealed that the grain size had essentially remained constant (Table I). Thus, the present data demonstrate that the primary stage of creep is not caused by concurrent grain growth.

A review of earlier work on polycrystalline alumina indicates that a primary stage of creep was observed in most, but not all, studies [9]. A possible explanation for this discrepancy is the differences in test temperatures employed in earlier studies. Davies and Sinha Ray [5] noted that increasing the test temperature had an effect of decreasing the extent of primary creep and Davies [17] reported that creep deformation at a temperature of 1973 K did not involve a primary stage of creep. Inspection of earlier investigations on polycrystalline alumina indicates that, generally, studies reporting a lack of a primary stage of creep were performed at temperatures greater than 1873 K.

4.1.1. Effect of concurrent grain growth

An inspection of Fig. 2 indicates that at stresses less than about 20 MPa, the strain rate continues to decrease at large strain levels. The grain growth data presented in Table I indicates that at low stresses,

grain growth had occurred to a considerable extent. It is therefore proposed that the observed decrease in strain rate at large strain levels is a direct consequence of concurrent grain growth during deformation at low stresses. It is also noted that the observation of a well-defined steady-state at a stress level of 75.5 MPa (Fig. 1) is consistent with the lack of grain growth at that stress level (Table I).

4.2. Activation energy for creep deformation

The apparent activation energy for the rate-controlling deformation process was obtained from an Arrhenius plot of the steady-state strain rates against reciprocal temperature (Fig. 3). Similar procedures [1, 17], temperature-cycling procedures [4, 5] and an evaluation based on a creep rate equation [1, 3] have been used earlier to determine apparent activation energies for creep in polycrystalline alumina. However, in order to identify the rate-controlling mechanism, it is necessary to compare the true activation energy for creep deformation with known values of the lattice and grain boundary anion and cation diffusivities.

The apparent activation energy is given by the following expression:

$$Q_a = -R\partial \ln \dot{\varepsilon}/\partial(1/T) \quad (2)$$

whereas the true activation energy is given by the expression:

$$Q_t = -R\partial \ln D/\partial(1/T) \quad (3)$$

where the diffusivity D is given as $D = D_0 \exp(-Q/RT)$.

By combining Equations 1 to 3, the relationship between the apparent and the true values of the activation energy is

$$Q_t = Q_a + RT - [(1 - n)RT^2/G]\mathrm{d}G/\mathrm{d}T \quad (4)$$

The value of the shear modulus G_T at a temperature T was determined from the relationship: $G_T = G_0 - (\mathrm{d}G/\mathrm{d}T)T$. Using published values of $G_0 = 1.7 \times 10^5$ MPa and $\mathrm{d}G/\mathrm{d}T = 23\,\mathrm{MPa\,K^{-1}}$ [18], the shear modulus at a temperature of 1673 K was estimated to be 1.3×10^5 MPa. The true activation energy for creep deformation at a temperature of 1673 K may therefore be determined by substituting $Q_a = 625\,\mathrm{kJ\,mol^{-1}}$, $G_{1673} = 1.3 \times 10^5$ MPa and $n = 1.9$ into Equation 4. This yields a true activation energy, Q_t, of $635\,\mathrm{kJ\,mol^{-1}}$.

This activation energy is in reasonable agreement with those reported earlier for the creep deformation of polycrystalline alumina [2, 9]. Within the limits of accuracy of these measurements, the activation energy for creep deformation is also similar to the activation energy for cation diffusion through the lattice [19]. The activation energy for cation grain boundary diffusion in alumina has not been determined explicitly although it has been inferred from earlier creep experiments to be $420\,\mathrm{kJ\,mol^{-1}}$ [2], which is less than the value obtained in this study.

4.3. Identification of the rate-controlling mechanism for steady state creep

Heuer *et al.* [1] reported that the stress exponents in early studies were typically of the order of $\simeq 1.1$ to 1.7 and the non-Newtonian behaviour was attributed to grain boundary sliding [1]. Davies and Sinha Ray [5] observed a transition from a stress exponent of 1 to a stress exponent of 2 with increasing stress. The stress exponent of 1 was attributed to Nabarro–Herring creep [14, 20] and it was suggested that the stress exponent of 2 resulted from a combination of Nabarro–Herring creep and an intragranular dislocation creep process [5]. Cannon *et al.* [6] observed a decrease in stress exponent from $\simeq 1.7$ at low stresses to $\simeq 1$ at high stresses; the stress exponent of $\simeq 1.7$ in this case was attributed to an interface-controlled creep mechanism. Porter *et al.* [21] examined the effect of concurrent cavitation on the stress exponent and this analysis indicated that the observed non-linearity in the stress exponent could not be explained on the basis of concurrent cavitation. Ikuma and Gordon [7, 8] developed conditions for the occurrence of interface controlled diffusional creep and the results of the present study will be analysed now in terms of diffusional and interface controlled creep mechanisms.

4.3.1. Diffusional creep mechanisms

Diffusional creep mechanisms involving the flow of vacancies through the lattice and along grain boundaries are respectively termed Nabarro–Herring [14, 20] and Coble creep [22]. In ionic materials, the diffusional creep process is controlled by the movement of the rate limiting species diffusing along the least resistant diffusion path [23]. In polycrystalline alumina, the available evidence suggests that anion diffusion occurs with least resistance [2] and hence it is anticipated that the creep process will be controlled by cation diffusion.

For cation diffusion control in alumina, the Nabarro–Herring creep rate is given by:

$$\dot{\varepsilon} = 40(\Omega_v D_l^+/2kTd^2)\sigma \quad (5)$$

where Ω_v is the molecular volume, D_l is the cation lattice diffusivity and the factor of 2 in the denominator corresponds to the valency of the anion in alumina. An evaluation of Equation 5, for $d = 1.6\ \mu$m, $\Omega_v = 4.5 \times 10^{29}\,\mathrm{m^3}$, $T = 1673$ K and $D_l^+ = 2.8 \times 10^{-4}\exp(-478000/8.3\,T)\,\mathrm{m^2 sec^{-1}}$ [19], is superimposed on to the stress–strain data obtained in this study (Fig. 2). Inspection of Fig. 2 indicates that, under the present experimental conditions, the Nabarro–Herring creep mechanism did not contribute significantly to the deformation of polycrystalline alumina.

The Coble creep mechanism [22], for cation diffusion control, predicts the following expression for the strain rate:

$$\dot{\varepsilon} = (48\Omega_v \delta D_{gb}^+/2kTd^3)\sigma \quad (6)$$

where δ is the effective width of the grain boundary, D_{gb}^+ is the cation grain boundary diffusivity and the factor of 2 in the denominator again corresponds to the anion valency. The value of δD_{gb}^+ in alumina is not known from independent measurements but an analysis of creep data suggests that the grain boundary diffusivity may be expressed as follows [2]:

$$\delta D_{gb}^{+} = 8.6 \times 10^{-10} \exp(-418000/8.3T)\,m^3 sec^{-1} \quad (7)$$

Equation 6 was evaluated using $d = 1.6\,\mu m$, $T = 1673\,K$ and δD_{gb} given by Equation 7 and the computed Coble creep rate is also superimposed on to Fig. 2. An examination of Fig. 2 indicates that, under the present experimental conditions, the Coble creep mechanism leads to higher strain-rates than the Nabarro–Herring mechanism and it is also noted that the line representing the Coble creep mechanism intersects the line corresponding to the experimental data at a stress level of approximately 150 MPa.

Thus, it is clear that the present experimental results cannot be rationalized in terms of the known diffusional creep mechanisms.

4.3.2. Interface-controlled diffusional creep

Coble creep [22] essentially involves the creation, diffusion and annihilation of vacancies along grain boundaries. The model was developed with the assumption that grain boundaries act as perfect sources and sinks for vacancies. However, when the grain boundaries do not act as perfect sources and sinks for vacancies, the process of vacancy creation/annihilation could become rate controlling. This process is termed the interface controlled diffusional creep mechanism.

Inspection of Fig. 2 indicates that the experimentally observed creep rates are considerably slower than those anticipated from an occurrence of Coble creep. The present experimental results are therefore consistent with the operation of an interfacial controlled diffusional creep mechanism.

Ikuma and Gordon [7, 8] analysed interface controlled diffusional creep in ceramics for several limiting conditions. The following equation for creep was developed under the assumption that the same interfacial mechanism occurs sequentially with lattice and grain boundary diffusion and that anion diffusion is not rate limiting:

$$\dot{\varepsilon} = \frac{44\Omega_v \sigma}{\alpha k T d^2} \times \left[1 \Big/ \left(\frac{44}{K'd} + \frac{1}{(D_l^{+}/\pi) + (\delta D_{gb}^{+}/d)}\right)\right] \quad (8)$$

where α is the cation valency and K' is the reaction rate constant.

From Equation 8, it follows that interface control will occur when:

$$\frac{44}{K'd} \ll \frac{1}{(D_l^{+}/\pi) + (\delta D_{gb}^{+}/d)} \quad (9)$$

Substituting the value of $d = 1.6\,\mu m$, $T = 1673\,K$, D_l^{+} [19] and δ_{gb}^{+} given by Equation 7, the criterion for the occurrence of interface controlled diffusional creep is given by:

$$K' \gg 10^{-9}\,m\,sec^{-1} \quad (10)$$

It is not possible to precisely define the experimental conditions under which interface controlled diffusion creep will occur because of a lack of knowledge of the explicit dependence of K' on factors such as stress, temperature and grain size. However, it is clear that, if an interface controlled mechanism is to explain the present experimental stress exponent, $K' \propto \sigma$.

Finally, it is important to emphasize that the concept of an interfacial controlled creep mechanism can be used to rationalize experimental results only when the experimental creep rates are slower than those predicted by the diffusional creep mechanisms. Thus, for example, it is possible to interpret the data of Cannon *et al.* [6] in terms of an interfacial controlled creep mechanism. On the other hand, it is not possible to attribute a stress exponent of 2 reported by Davies and Sinha Ray [5] to an interfacial controlled creep mechanism because their experimental creep rates under such conditions were faster than the experimentally observed diffusional creep rates.

5. Summary and conclusions

1. Normal primary creep transients were observed up to strains of $\simeq 1\%$. It was shown that grain growth cannot account for the occurrence of the primary creep stages in which the creep rate decreased with deformation

2. A true activation energy of $635\,kJ\,mol^{-1}$ was obtained in the analysis, which is in reasonable agreement with the activation energy for cation lattice diffusion and higher than that for cation grain boundary diffusion.

3. At high stresses, well defined steady-state conditions were obtained beyond strains of $\simeq 2\%$, whereas at low stresses, the strain-rates continued to decline at large strains. These results were rationalized in terms of concurrent grain growth at low stresses.

4. The stress exponent for creep was determined to be 1.9. The experimental strain-rates were slower than the theoretical predictions of the Coble creep mechanism. Thus, the creep deformation is consistent with an interface controlled diffusional creep mechanism.

Acknowledgement

The authors wish to acknowledge the support of the National Science Foundation under Grant No. DMR 8217120.

References

1. A. H. HEUER, R. M. CANNON and N. J. TIGHE, "Ultrafine-Grain Ceramics" edited by J. J. Burke, N. L. Reed and V. Weiss (Syracuse University Press, Syracuse, New York, 1970) p. 339.
2. R. M. CANNON and R. L. COBLE, "Deformation of Ceramic Materials", edited by R. C. Bradt and R. E. Tressler (Plenum, New York, 1975) p. 61.
3. R. C. FOLWEILER, *J. Appl. Phys.* **32** (1961) 773.
4. G. M. FRYER and J. P. ROBERTS, *Proc. Brit. Ceram. Soc.* **6** (1966) 225.
5. C. K. L. DAVIES and S. K. SINHA RAY, "Special Ceramics" edited by P. Popper (British Ceramic Research Association, Stoke-on-Trent, 1972) p. 193.
6. R. M. CANNON, W. H. RHODES and A. H. HEUR, *J. Amer. Ceram. Soc.* **63** (1980) 46.
7. Y. IKUMA and R. S. GORDON, in "Surfaces and Interfaces in Ceramic and Ceramic–Metal Systems", edited by J. A. Pask and A. G. Evans (Plenum, New York, 1981) p. 283.
8. *Idem, J. Amer. Ceram. Soc.* **66** (1983) 139.

9. W. R. CANNON and T. G. LANGDON, *J. Mater. Sci.* **18** (1983) 1.
10. J. A. STAVRIOLAKIS and F. H. NORTON, *J. Amer. Ceram. Soc.* **33** (1950) 263.
11. G. W. HOLLENBERG, G. R. TERWILLIGER and R. S. GORDON, *ibid.* **54** (1971) 196.
12. P. YAVARI and T. G. LANGDON, in "Surfaces and Interfaces in Ceramic and Ceramic–Metal Systems", edited by J. A. Pask and A. G. Evans (Plenum, New York, 1981) p. 295.
13. A. H. HEUER, N. J. TIGHE and R. M. CANNON, *J. Amer. Ceram. Soc.* **63** (1980) 53.
14. C. HERRING, *J. Appl. Phys.* **21** (1950) 437.
15. I. M. LIFSHITS, *Soc. Phys. JETP* **17** (1963) 909.
16. I. M. LIFSHITS and V. B. SHIKIN, *Sov. Phys. Solid State* **6** (1964) 1362.
17. C. K. L. DAVIES, in "Physical Metallurgy of Reactor Fuel Elements", edited by J. E. Harris and E. C. Sykes (The Metals Society, London, 1975) p. 99.
18. D. H. CHUNG and G. SIMMONS, *J. Appl. Phys.* **39** (1968) 5316.
19. A. E. PALADINO and W. D. KINGERY, *J. Chem. Phys.* **37** (1962) 957.
20. F. R. N. NABARRO, "Report of a Conference on the Strength of Solids" (The Physical Society, London, 1948) p. 75.
21. J. R. PORTER, W. BLUMENTHAL and A. G. EVANS, *Acta Metall.* **29** (1981) 1899.
22. R. L. COBLE, *J. Appl. Phys.* **34** (1963) 1679.
23. R. S. GORDON, *J. Amer. Ceram. Soc.* **56** (1973) 147.

Received 29 January
and accepted 1 May 1985